Determination of the phase difference between the Raman tensor elements of the A_{1g}-like phonons in $SmBa_2Cu_3O_{7-\delta}$

T. Strach, J. Brunen, B. Lederle, J. Zegenhagen, and M. Cardona
Max-Planck-Institut für Festkörperforschung, Heisenbergstr. 1, 70569 Stuttgart, Germany
(Received 8 August 1997)

We describe a general method to determine the relative phase difference between the complex components of a phononic Raman tensor from the measured angular dependence of the intensity of light scattered inelastically by the phonon in a Raman process. The method is applied to Raman spectra of a (110)-oriented $SmBa_2Cu_3O_{7-\delta}$ thin film obtained at room temperature. From our spectra we derive for the A_{1g}-like phonons the anisotropy ratio and the relative phase difference between the two independent components of the Raman tensor as a function of laser energy $\hbar\omega$. We point out that our results can be used to verify theoretical calculations of Raman tensors and compare our data with values calculated for the related compound $YBa_2Cu_4O_8$. [S0163-1829(98)02202-4]

I. INTRODUCTION

Raman scattering by phonons has yielded important information about the physical properties of the high-T_c superconductors.[1,2] Phonons can be classified and identified in a Raman experiment by the dependence of their intensity on incident and scattered light polarizations.[3,4] If several phonons share the same polarization behavior, as is often the case in the high-T_c materials, Raman studies on isotopically engineered samples may be used to determine the exact phonon eigenvector belonging to each of the observed vibrations.[5–9] In addition to this, phononic Raman scattering also allows one to investigate indirectly the electronic spectrum of a high-T_c superconductor via the self-energies induced by the electron-phonon interaction. From changes in the observed frequencies, widths, and asymmetries of phononic Raman lines, conclusions can be drawn about corresponding changes in the electronic spectrum.[10,11] As an example, the existence of a superconducting gap with an energy of $2\Delta=(5.0\pm0.15)k_BT_c$ was early inferred from *phononic* Raman scattering experiments in $RBa_2Cu_3O_{7-\delta}$ ($R=Y$, most rare earths).[12]

However, Raman scattering by phonons incorporates a more subtle connection between the phononic and the electronic system of a material than the self-energies mentioned above. The main contribution to inelastic light scattering by phonons does not originate from a direct photon-phonon interaction, but from a three-step process which involves two virtual electronic excitations as intermediate states.[13] The scattering process, i.e., the creation or annihilation of a phonon, takes place as the transitional step between two virtual electronic excitations. This transitional step is effected by the electron-phonon interaction. Phononic Raman scattering is thus always closely linked to the electronic system of the solid.

The properties of a phonon with respect to Raman scattering are described by its Raman tensor $\vec{R}$, a quantity which is represented by a complex 3×3 matrix. For incident and scattered light with polarization vectors $\hat{e}_l$ and $\hat{e}_s$, respectively, the intensity I of a phononic Raman process is given by[13]

$$I\sim|\hat{e}_s\cdot\vec{R}\cdot\hat{e}_l|^2. \tag{1.1}$$

From the symmetry properties of the phonon one can deduce the number of independent Raman tensor components, which is normally much smaller than the total number of nine elements. In the case of an A_{1g} phonon in a tetragonal material, for example, the number of independent components is only two ($R_{xx}=R_{yy}$ and R_{zz}). It can be shown that if neither the energy of the incoming nor of the scattered light is in resonance with an electronic interband excitation of the solid, the Raman tensor may be expressed as the partial derivative of the dielectric tensor $\vec{\epsilon}(\omega)$ of the material with respect to the phonon normal coordinate Q of the vibration:[13]

$$\vec{R}(\omega)\sim\frac{\partial\vec{\epsilon}(\omega)}{\partial Q}. \tag{1.2}$$

Here ω denotes the frequency of the incoming laser light, *not* the frequency of the phonon. Using Eq. (1.2) the Raman scattering efficieny of a phonon can be calculated as a function of laser energy and compared to results from Raman scattering experiments. This has indeed been successfully done for $YBa_2Cu_3O_{7-\delta}$, where absolute Raman scattering efficiencies for the five prominent phonons with orthorhombic A_g symmetry have been measured and compared to first principles calculations based on atomic sphere approximation (ASA) linear muffin-tin orbital (LMTO) band structures.[14]

The dielectric tensor $\vec{\epsilon}(\omega)$ of a material is a complex function, and thus the Raman tensor, as its partial derivative, is in general also complex. This property of the Raman tensor is commonly not exploited in experiments; measuring the Raman intensity of a phonon with polarization vectors of incident and scattered light along the main axes x, y, or z of the Raman tensor corresponds to the determination of the *absolute* value of one tensor component only. The phase information is lost in the measuring process. This is different, however, in other scattering geometries, where $\hat{e}_l$ and $\hat{e}_s$ are

not parallel to the main axes of $\vec{\vec{R}}$. In these cases, the *relative* phase difference between Raman tensor elements influences the strength of the scattering process. The phase difference can therefore be determined experimentally from such types of measurements. For a comparison with theoretical calculations, the knowledge of this quantity is, of course, desirable.

In this paper we present room temperature Raman spectra of a (110)-oriented $SmBa_2Cu_3O_{7-\delta}$ film for different scattering geometries. From these spectra we derive the anisotropy ratio and, for the first time to our knowledge, the phase difference between the two independent Raman tensor elements for the A_{1g}-like phonons in this material as a function of laser energy. The results will be compared with previous resonant Raman scattering experiments on $YBa_2Cu_3O_{7-\delta}$ and theoretical predictions obtained for the related compound $YBa_2Cu_4O_8$.

II. THEORY

The Raman tensor of a phonon with A_{1g} symmetry in a tetragonal material is[13]

$$\vec{\vec{R}}_{A_{1g}}=\begin{pmatrix} a & & \\ & a & \\ & & c \end{pmatrix}=\begin{pmatrix} |a|e^{i\varphi_a} & & \\ & |a|e^{i\varphi_a} & \\ & & |c|e^{i\varphi_c} \end{pmatrix}, \tag{2.1}$$

where $|a|$, φ_a, $|c|$, and φ_c represent magnitude and complex phase of the two independent components of the tensor, respectively ($R_{xx}=R_{yy}$). For Raman backscattering experiments on a (110) surface the polarization vectors of incident and scattered light referred to the tetragonal axes may be written as

$$\hat{e}_{l,s}=\begin{pmatrix} -\frac{1}{\sqrt{2}}\sin(\vartheta_{l,s}) \\ \frac{1}{\sqrt{2}}\sin(\vartheta_{l,s}) \\ \cos(\vartheta_{l,s}) \end{pmatrix}, \tag{2.2}$$

where $\vartheta_{l,s}$ denotes the angle between the z axis of the sample and the polarization vector of the light. We will limit our discussion to parallel ($\vartheta_s=\vartheta_l$) and perpendicular ($\vartheta_s=\vartheta_l+90°$) scattering configurations. For these two special cases Eq. (1.1) yields the Raman intensities

$$I_{\parallel}(\vartheta)\sim|a|^2\sin^4(\vartheta)+|c|^2\cos^4(\vartheta) +2|a||c|\cos(\varphi_{ac})\sin^2(\vartheta)\cos^2(\vartheta) \tag{2.3}$$

and

$$I_{\perp}(\vartheta)\sim[|a|^2+|c|^2-2|a||c|\cos(\varphi_{ac})]\sin^2(\vartheta)\cos^2(\vartheta), \tag{2.4}$$

with $\vartheta=\vartheta_l$ and $\varphi_{ac}=\varphi_a-\varphi_c$. Figure 1 displays $I_{\parallel}(\vartheta)$ for one particular choice of values $|a|$ and $|c|$ and several different phase angles φ_{ac}. It can be seen that the dependence of $I_{\parallel}$ on ϑ varies strongly with the phase angle φ_{ac}. While the value of $I_{\parallel}(\vartheta)$ at $\vartheta=0°$ and $\vartheta=90°$ is given by $|c|^2$ and $|a|^2$, respectively, for intermediate angles it also depends on the parameter φ_{ac}. Thus the function $I_{\parallel}(\vartheta)$ is unique for any particular choice of $|a|,|c|$, and φ_{ac} and allows an unambiguous determination of all three parameters. This is not true for $I_{\perp}(\vartheta)$, where different sets of parameters $|a|,|c|$, and φ_{ac} may produce identical line shapes. Nevertheless, $I_{\perp}(\vartheta)$ is still useful as a consistency check for parameters obtained from an evaluation of $I_{\parallel}(\vartheta)$.

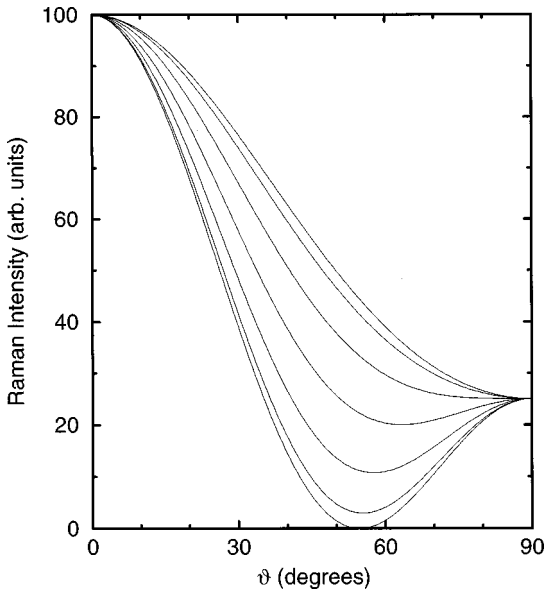

FIG. 1. Calculated Raman intensity $I_{\parallel}(\vartheta)$ according to Eq. (2.3) for a tetragonal A_{1g} phonon measured on a (110) surface of the material. ϑ represents the angle between the z axis of the sample and the polarization vector of incident and scattered light. The values for the parameters $|a|$ and $|c|$ are 5 and 10, respectively, for all curves. The values of φ_{ac} range from 0 (top curve) to π (bottom curve) in steps of $\pi/6$.

III. EXPERIMENT

The sample used in this study is a (110)-oriented $SmBa_2Cu_3O_{7-\delta}$ thin film grown on top of a $PrBa_2Cu_3O_{7-\delta}$ buffer layer on a (110)-oriented $SrTiO_3$ substrate using pulsed laser deposition.[15] The z axis of the film is aligned in the film plane along the [001] substrate direction, while the x and y axes point out of the film surface under angles of 45°. The film is twinned in the xy plane and thus appears pseudotetragonal in a macroscopic Raman experiment.

Raman spectra have been recorded at room temperature in a near-backscattering geometry. The film was located in a vacuum chamber to prevent Raman scattering from air molecules. All measurements were performed either in parallel ($\vartheta_s=\vartheta_l$) or perpendicular ($\vartheta_s=\vartheta_l+\pi/2$) polarization for various angles ϑ_l between the z axis of the film and the polarization vector of the incoming laser light. The backscattered light was analyzed with a double monochromator equipped with a liquid nitrogen cooled charge-coupled-device (CCD) detector. Various laser lines of a Kr-Ar mixed gas laser were used for excitation. The laser beam was focused onto a ≈50-μm-diam spot on the sample surface and the laser power was kept between 25 and 50 mW.

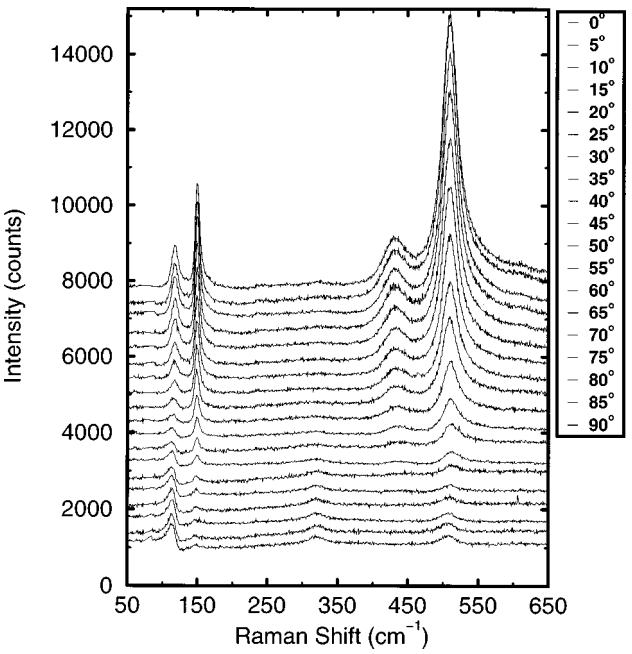

FIG. 2. Room temperature Raman spectra of a (110)-oriented $SmBa_2Cu_3O_{7-\delta}$ thin film taken in parallel polarization ($\hat{e}_s=\hat{e}_l$). The spectra have been measured for various angles ϑ between the z axis of the sample and the polarization vector $\hat{e}_l$ of the incident laser light, ranging from $\vartheta=0°$ (top curve) to 90° (bottom curve) in steps of 5°. The laser wavelength used is 514.5 nm and the recording time is 300 s for all spectra.

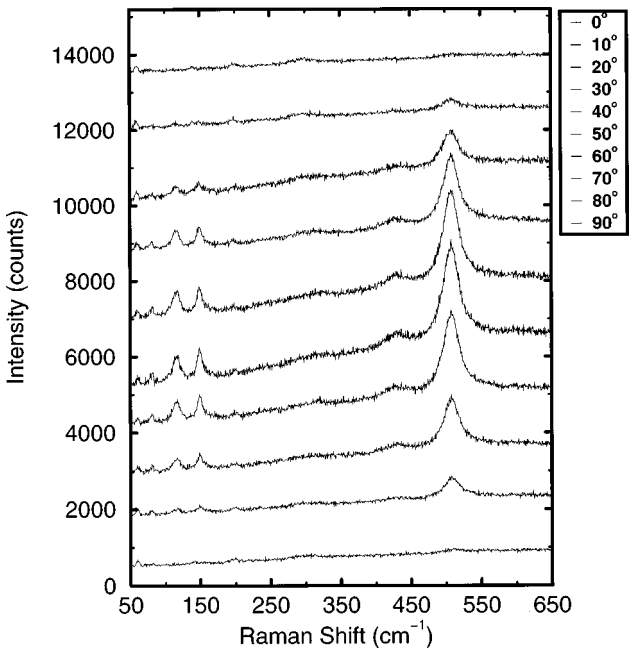

FIG. 3. Room temperature Raman spectra of a (110)-oriented $SmBa_2Cu_3O_{7-\delta}$ thin film in crossed polarization ($\hat{e}_s=\hat{e}_l+90°$). The spectra correspond to different angles ranging from $\vartheta=0°$ (top curve) to 90° (bottom curve) in steps of 10°. The recording time is 300 s and the laser wavelength is 514.5 nm for all spectra.

IV. RESULTS

Figure 2 shows room temperature Raman spectra of the $SmBa_2Cu_3O_{7-\delta}$ (110) film in parallel polarization for different angles ϑ obtained with the green laser line (2.43 eV). The Raman lines for the four phonons with tetragonal A_{1g} symmetry are clearly visible at 114, 146, 428, and 506 cm^{-1}. They correspond to the motion along the z axis of the Ba, Cu(2), O(2)+O(3), and O(4) atoms, respectively.[1] The out-of-phase O(2)-O(3) phonon (tetragonal B_{1g} symmetry) also shows up as a weak feature around 320 cm^{-1} for angles ϑ close to 90°. The appearance of this line, which is forbidden by symmetry in this scattering geometry for a truly tetragonal material, may either reflect the microscopic orthorhombicity of the film or indicate the existence of a small fraction of $SmBa_2Cu_3O_{7-\delta}$ grown in a different crystallographic orientation. All phonons drastically change their intensity with angle ϑ. The Cu(2), O(2)+O(3), and O(4) phonons continuously lose Raman intensity with increasing angle; the O(2)+O(3) phonon at 440 cm^{-1} becomes so weak that it cannot be observed above $\vartheta=80°$. The intensity of the Ba phonon at 115 cm^{-1}, on the other hand, reaches a minimum for $\vartheta\approx45°$ and then increases again. This phonon also exhibits a pronounced change in its line shape: While it has a symmetric shape with a Lorentzian line profile for $\vartheta=0°$, it appears strongly asymmetric[16] with a Fano line shape for angles $\vartheta>45°$.

Raman spectra of the same film measured at room temperature in crossed polarization are shown in Fig. 3. In this polarization geometry the intensity of all four A_{1g}-like phonons vanishes for $\vartheta=0°$ and 90° and is largest for $\vartheta=45°$.

We extracted the intensity of the phonons from our Raman spectra by means of numerical line fits. The Cu(2), O(2)+O(3), and O(4) phonons were fitted with Lorentzians, while we used a Fano profile for the Ba phonon.[17] The result of this procedure for the spectra measured in parallel polarization is displayed in Fig. 4. The intensity of the four A_{1g}-like phonons in crossed polarization as a function of polarization angle ϑ is shown in Fig. 5.

Using Eq. (2.3) we determined the three unknown parameters $|a|$, $|c|$, and φ_{ac} from the angular dependence $I_\parallel(\vartheta)$ of the Raman intensity measured for each phonon. Again a least squares fit procedure was used to extract the parameters. In order to avoid confusion and to stress the difference between the polarization *angle* ϑ and the complex phase *difference* φ_{ac} all subsequent values for φ_{ac} will be given in units of radians, while values for ϑ will always be given in degrees. The functions which yield the best fit are displayed as solid lines in Fig. 4. In addition, two more lines are shown, which correspond to functions $I_\parallel(\vartheta)$ with the same values for $|a|$ and $|c|$, but extremal phase shifts of $\varphi_{ac}=0$ (dashed line) and $\varphi_{ac}=\pi$ (dotted line). These additional curves have been drawn to give a feeling for the sensitivity of the overall line shape of $I_\parallel(\vartheta)$ with respect to the phase difference φ_{ac}. The best fit curve can clearly be distinguished from either extremal curve for the Ba, Cu(2), and O(4) phonons. This is not true, however, in the case of the O(2)+O(3) phonon. For this phonon all phase shifts produce nearly identical intensity functions $I_\parallel(\vartheta)$, so that φ_{ac} cannot be extracted accurately from the experimental data in this case. The reason for the insensitivity is the very small value of the Raman tensor element $|a|$ of the O(2)+O(3) phonon. Since the dependence of $I_\parallel(\vartheta)$ on the phase difference φ_{ac} in Eq. (2.3) originates from a term which is proportional to the product of $|a|$ and

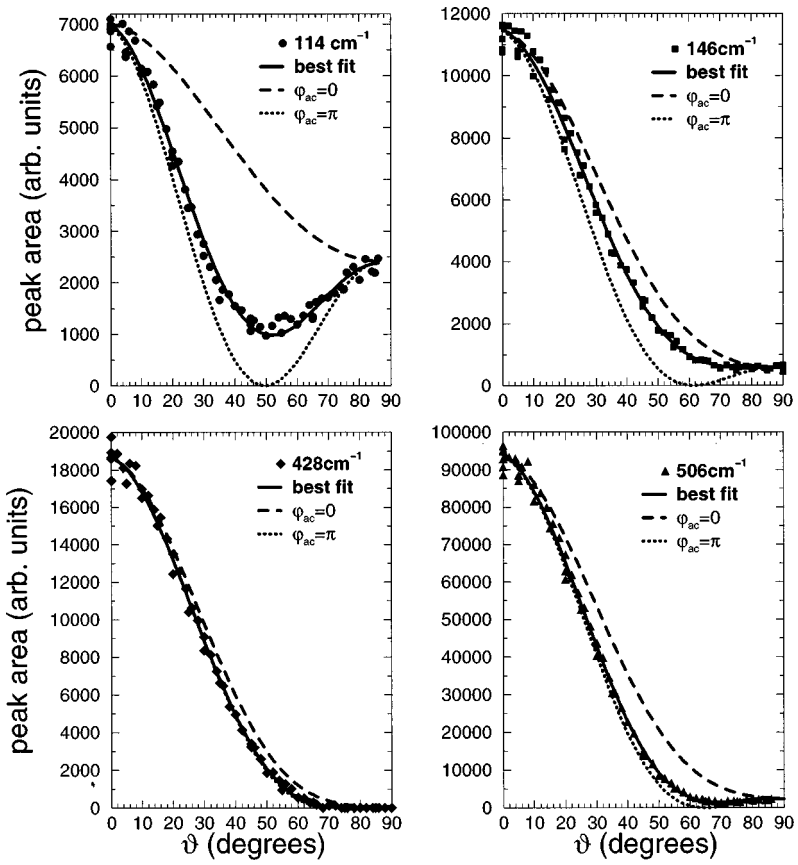

FIG. 4. Raman intensities $I_{\parallel}(\vartheta)$ of the four A_{1g}-like phonons of $SmBa_2Cu_3O_{7-\delta}$ at room temperature on a (110) surface in parallel polarization as function of angle ϑ. Solid symbols correspond to experimental values determined from the spectra by numerical line fits. Solid lines represent the results of a least squares fit of Eq. (2.3) to the data. The best fit values for φ_{ac} are 2.08, 1.45, 2.58, and 2.21 for the Ba, Cu(2), O(2)+O(3), and O(4) phonons, respectively. The dashed and dotted lines show intensity functions using the same values $|a|$ and $|c|$ as determined for the best fit, but phase shifts of $\varphi_{ac}=0$ and $\varphi_{ac}=\pi$, respectively.

$|c|$, it must necessarily vanish if one of the two components approaches zero.

As a consistency check we have calculated the functions $I_{\perp}(\vartheta)$ for the four A_{1g}-like phonons using Eq. (2.4) and the parameters obtained from the fits of $I_{\parallel}(\vartheta)$. The calculated curves agree very well with our measurements for the Ba, Cu(2), and O(4) phonons, while in the case of the O(2) +O(3) phonon the agreement between experiment and calculation is better for a phase difference of $\varphi_{ac}=0$ than for the phase difference found from the fit to $I_{\parallel}(\vartheta)$.

We have repeated the procedure outlined above for several wavelengths of the incident laser light and determined anisotropy $|a|/|c|$ and phase difference φ_{ac} as well as the relative strength for the four A_{1g}-like phonons as a function of laser energy. The results of our measurements are summarized in Fig. 6. To compare the relative intensities of the phonons, Fig. 6(a) displays the Raman tensor coefficients R_{zz} of the Ba, Cu, and O(2)+O(3) phonons normalized with respect to the strongest coefficient R_{zz}(O(4)). The coefficients have been corrected for the Bose-Einstein thermal population factor at 300 K in order to refer them to 0 K. Figure 6(b) shows the anisotropy ratios $|a|/|c|$ obtained in this manner for all four phonons. Figure 6(c) displays the phase difference φ_{ac} between the tensor elements R_{xx} and R_{zz} for each of the phonons. Since only the cosine of the phase difference enters in Eqs. (2.3) and (2.4), the sign of φ_{ac} cannot be determined from these experiments and has been chosen arbitrarily to be positive in all cases.

V. ANALYSIS AND DISCUSSION

Besides small differences in the positions of the phonon lines, the overall shape of the Raman signal does not change very much upon replacement of Sm by Y in $RBa_2Cu_3O_{7-\delta}$. We thus compare our results to Raman experiments of Heyen *et al.*[14] and Misochko and Sherman[18] performed on $YBa_2Cu_3O_{7-\delta}$. The relative intensities in zz polarization [Fig. 6(a)] as well as the $|a|/|c|$ anisotropies [Fig. 6(b)] are in fair agreement with the ones determined in $YBa_2Cu_3O_{7-\delta}$. In both materials the by far largest scattering intensity is found for the O(4) phonon in zz polarization, while the intensity of the other phonons is considerably smaller. The large $|a|/|c|$ anisotropies of the oxygen related phonons are also found in both materials, leading to intensity ratios I_{zz}/I_{xx} of more than 25:1 at all laser energies. The most prominent difference between $YBa_2Cu_3O_{7-\delta}$ and $SmBa_2Cu_3O_{7-\delta}$ occurs for the Ba phonon which in $YBa_2Cu_3O_{7-\delta}$ shows almost no Raman intensity in zz polarization for incident laser energies around 2.2 eV, thus leading to anisotropy ratios $|a|/|c|$ much larger than unity. This is not the case in $SmBa_2Cu_3O_{7-\delta}$. In this material the intensity of the Ba phonon in zz polarization does not have a

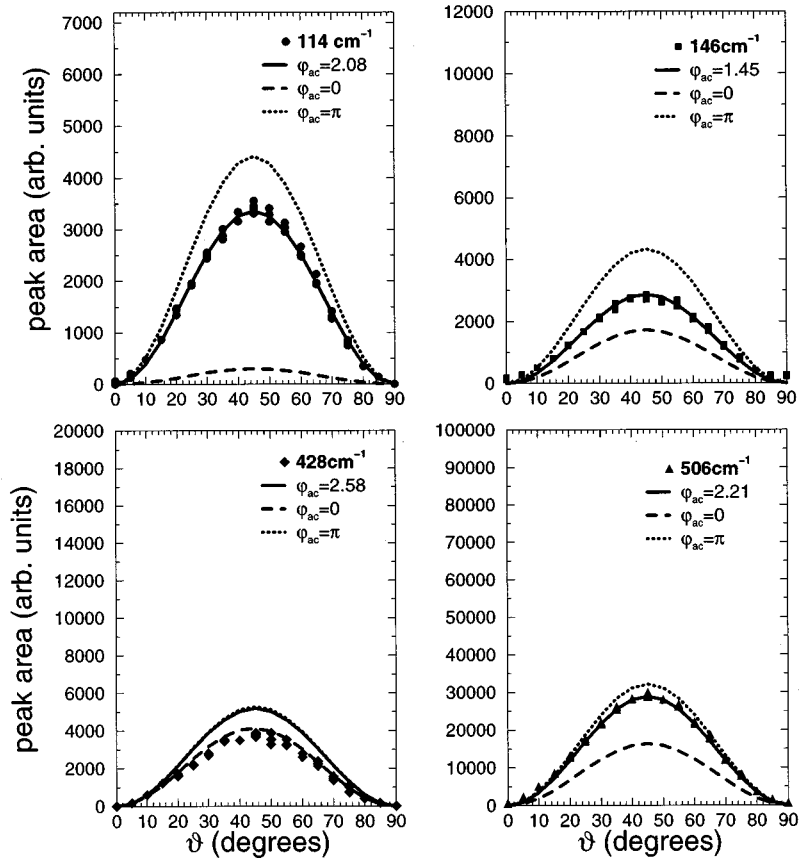

FIG. 5. Raman intensities $I_{\perp}(\vartheta)$ of the four A_{1g}-like phonons of $SmBa_2Cu_3O_{7-\delta}$ at room temperature on a (110) surface in crossed polarization as function of angle ϑ. Symbols correspond to experimental results; the solid, dotted, and dashed lines represent intensity profiles according to Eq. (2.4) with the same parameters $|a|$,$|c|$, and φ_{ac} as in Fig. 4.

pronounced minimum at this energy. Therefore the $|a|/|c|$ ratio remains below 1.0 at all energies in $SmBa_2Cu_3O_{7-\delta}$ and shows only a weak maximum at 2.2 eV.

Figure 6(c) indicates that the phase difference φ_{ac} for a given phonon does not vary strongly with laser energy. For the Ba, the O(2)+O(3) and O(4) phonons the phase differences range from 0.5π to 0.75π, with a minimum at 2.2 eV. The Cu(2) phonon exhibits phase differences of less than 0.5π at all laser energies, with the maximum value around 2.35 eV. These numbers should be useful to test the results of future theoretical calculations of Raman efficiencies of phonons in $SmBa_2Cu_3O_{7-\delta}$ or related materials. As a first example we show in Fig. 7 theoretical values for the phase difference and anisotropy ratio of Cu and Ba phonons in the related orthorhombic compound $YBa_2Cu_4O_8$ as obtained recently from LMTO-ASA calculations.[19] Because of the orthorhombicity, the two Raman tensor elements R_{xx} and R_{yy} have different values in this material. In the case of the Ba phonon, R_{xx} and R_{yy} are comparable in magnitude. We display anisotropy ratios and phase shifts for both tensor elements. For the Cu phonon the calculation yields values for R_{xx} that are larger by at least a factor of two than the corresponding values for R_{yy}. We have therefore only plotted the anisotropy ratio and the phase difference between R_{xx} and R_{zz}. In all cases the calculated values are in qualitative agreement with the results obtained on the twinned, pseudotetragonal $SmBa_2Cu_3O_{7-\delta}$ film.

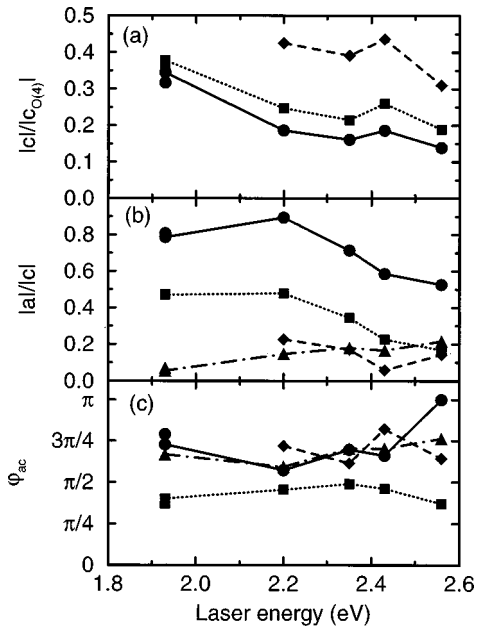

FIG. 6. Relative values $|c|/|c_{O(4)}|$, anisotropy ratios $|a|/|c|$, and phase difference angles φ_{ac} for the A_{1g}-like phonons in $SmBa_2Cu_3O_{7-\delta}$ as a function of incident laser energy. The symbols correspond to Ba (circles, solid lines), Cu(2) (squares, dotted lines), O(2)+O(3) (diamonds, dashed lines), and O(4) (triangles, long dashed lines) phonons, respectively.

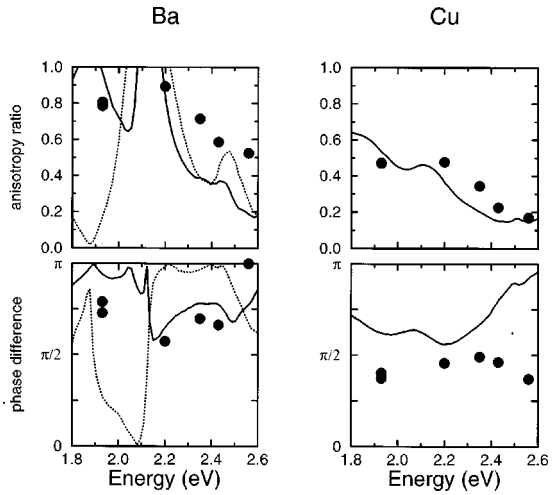

FIG. 7. Calculated anisotropy ratios $|a|/|c|$, $|b|/|c|$ and phase differences $\varphi_{ac}, \varphi_{bc}$ for the Ba and Cu(2) phonons in $YBa_2Cu_4O_8$ (solid and dashed lines) compared to experimental values obtained on a $SmBa_2Cu_3O_{7-\delta}$ film (dots). The solid and dotted lines correspond to parameters obtained in x direction (perpendicular to the Cu-O chains, $|a|/|c|$ and φ_{ac}) and in the y direction (parallel to the Cu-O chains, $|b|/|c|$ and φ_{bc}), respectively.

As mentioned above the calculation of absolute Raman scattering efficiencies for phonons in $YBa_2Cu_4O_8$ predicts that there is an appreciable anisotropy between the Raman tensor elements R_{xx} and R_{yy}. While the problem of in-plane anisotropy has not been addressed in this paper it would be interesting to repeat this type of experiment on the xy surface of an untwinned crystal to determine the phase difference $\varphi_a - \varphi_b$. Since the absolute values of R_{xx} and R_{yy} are comparable, the influence of the interference term should be at maximum and even small phase differences may be detectable. It should also be noted that the application of this method is not limited to any particular materials class, but applies generally to phononic Raman scattering in any noncubic crystalline solid.

VI. CONCLUSION

We have presented a general method to determine experimentally phase differences between two complex elements of a phononic Raman tensor. The method has been successfully applied to Raman spectra of a $SmBa_2Cu_3O_{7-\delta}$ (110)-oriented thin film, and the phase difference between the two independent Raman tensor elements a and c has been determined for the A_{1g}-like phonons. We have pointed out that this phase difference can be used as additional experimental quantity to verify theoretical calculations of the Raman tensor for a given phonon using band-structure-based first-principles calculations.

ACKNOWLEDGMENTS

We thank W. Stiepany, H. Hirt, and M. Siemers for technical assistance. Thanks are also due to V. Hadjiev for a careful reading of the manuscript.

[1] C. Thomsen, and M. Cardona, in *Physical Properties of High Temperature Superconductors I*, edited by D. M. Ginsberg (World Scientific, Singapore, 1989), p. 409, and references therein.

[2] C. Thomsen, in *Light Scattering in Solids VI*, edited by M. Cardona and G. Güntherodt (Springer, Berlin, 1991), p. 285.

[3] L. V. Gasparov, V. D. Kulakovskii, O. V. Misochko, and V. B. Timofeev, Physica C **157**, 341 (1989).

[4] K. F. McCarty, J. Z. Liu, R. N. Shelton, and H. B. Radousky, Phys. Rev. B **41**, 8792 (1990).

[5] A. Mascarenhas, H. Katayama-Yoshida, J. Pankove, and S. K. Deb, Phys. Rev. B **39**, 4699 (1989).

[6] J. C. Irvin, J. Chrzanowski, E. Altendorf, J. P. Franck, and J. Jung, J. Mater. Res. **5**, 2780 (1990).

[7] R. Henn, T. Strach, E. Schönherr, and M. Cardona, Phys. Rev. B **55**, 3285 (1997).

[8] G. A. Kourouklis, A. Jayaraman, B. Batlogg, R. J. Cava, M. Stavola, D. M. Krol, E. A. Rietman, and L.F. Schneemeyer, Phys. Rev. B **36**, 8320 (1987).

[9] D. Zech, H. Keller, K. A. Müller, K. Conder, E. Kaldis, E. Liarokapis, and N. Poulakis, Nature (London) **371**, 681 (1994).

[10] C. Thomsen, M. Cardona, R. Liu, B. Gegenheimer, and E. T. Heyen, Physica C **162–164**, 1079 (1989).

[11] R. Zeyher and G. Zwicknagl, Z. Phys. B **78**, 175 (1990).

[12] B. Friedl, C. Thomsen, and M. Cardona, Phys. Rev. Lett. **65**, 915 (1990).

[13] M. Cardona, in *Light Scattering in Solids II*, edited by M. Cardona and G. Güntherodt (Springer, Berlin, 1982), p. 19.

[14] E. T. Heyen, S. N. Rashkeev, I. I. Mazin, O. K. Andersen, R. Liu, M. Cardona, and O. Jepsen, Phys. Rev. Lett. **65**, 3048 (1990).

[15] J. Brunen, T. Strach, J. Zegenhagen, and M. Cardona, Physica C **282-287**, 599 (1997); Physica C **289**, 177 (1997).

[16] S. L. Cooper, M. V. Klein, B. G. Pazol, J. P. Rice, and D. M. Ginsberg, Phys. Rev. B **37**, 5920 (1988).

[17] *Light Scattering in Solids VI* (Ref. 2), p. 326.

[18] O. V. Misochko and E. Ya. Sherman, Sov. Phys. JETP **72**, 185 (1991).

[19] B. Lederle and M. Cardona (unpublished).